Period Determination of DY Pegasi

Dana Spiegel
January 27, 1999

ABSTRACT. DY Pegasi, a   Scuti or Dwarf Cepheid variable star, was observed. Using techniques of on-chip differential photometry, measurements of DY Pegasi and a non-variable comparison were collected. Relative V magnitude measurements were derived, showing a periodic variation in the V magnitude of DY Pegasi. Using Fourier analysis, a model was derived for this V magnitude variability. A period of 1.74 ± 0.04 hours per cycle was determined from the Fourier model.

1. INTRODUCTION

Variable stars are stars that pulsate in brightness, either regularly or irregularly. By observing the brightness of such a star over time and recording that brightness accurately the period of that star can be determined. Such a period determination can at the very least provide some model for the future behavior of a star if the star indeed pulsates on a regular basis. Period determination can also track the changing rate of pulsation of the star if its period is irregular.

Variable stars can be categorized into a small set of types, which include Cepheid variables and RR Lyrae variables.[1] These types are determined by their physical characteristics, one of which is the period of variability of brightness. By determining the pulsation period and light curve shape of a variable star, that star can usually be categorized into a particular type, although such a categorization is beyond the scope of this experiment.

This experiment aims to determine the pulsation period of the V magnitude of the known variable star DY Pegasi, a δ Scuti[2] (Dwarf Cepheid) variable star within the constellation Pegasus. Over the course of a night, the brightness of this star, along with the brightness of a comparison star, was measured using on-chip differential photometry. These data were then reduced, and the relative brightness of DY Pegasi as compared with this comparison star was determined over time. A Fourier series model was then fitted to the data and a period was determined from this model.

2. OBSERVATIONS

All observations were carried out at the Wallace Astronomical Observatory (ϕ =+42° 36'.37, λ =-71° 29'.1) in Westford, Massachusetts, using a 14-inch Celestron Schmidt-Cassegrain telescope. Images were captured by a Lynxx2000 CCD camera with a PFE-1 flip-mirror assembly and a 0.5x telecompressor lens. The CCD camera was attached to a Macintosh IIci computer running the appropriate Lynxx2000 32-bit image capture program. Observations were made on the night of October 20, 1998, from Universal Time 2^h31^m through 5^h10^m (see Appendix A for a complete list of observing times). 90-second exposure images of DY Pegasi [α =23^h 08^m 51^s, δ =+17° 12' 51".9 (J2000)] were taken at regular intervals during this time, for a total of 72 images.

Each image included a comparison star dubbed "Comp A" [α =23^h 08^m 51.^{m}538, δ =+17° 10' 49".116 (J2000)] (the
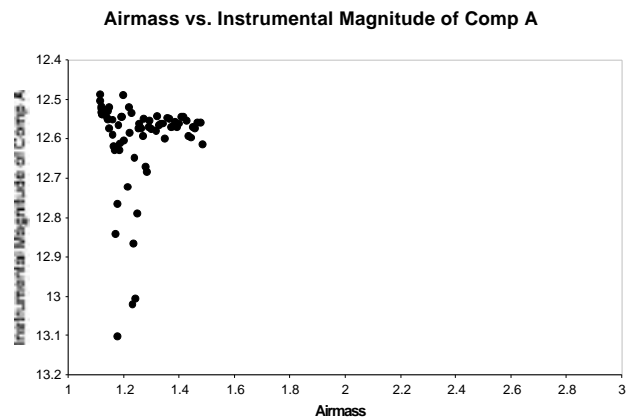

Figure 1. Instrumental Magnitude versus Airmass of Comp A. Note the small range of airmasses that are represented by the measurements of Comp A.

2

name Comp A is not the star's canonical name; it is used only for convenience in this report), which is believed to be non-variable or variable only in the long term. A comparison star's brightness can be compared to the object of interest's brightness to measure its relative brightness over time. To be an acceptable candidate for a comparison object, a star must either not vary in brightness or have a period of brightness variability that is significantly longer than that of the star being compared to it. If it is variable, the comparison star must have a brightness amplitude small enough that during the time of observation, the brightness of the comparison star doesn't change significantly. A star can also be used as a comparison star if its variability is modeled accurately enough to remove that variability from its brightness measurement, although this method introduces another set of errors.

90-second exposures provided signal from both DY Pegasi and Comp A that were more than 3000 pixel counts above noise, but not fully saturated, as determined by Lynxx2000 software analysis at the time of exposure. The rule-of-thumb used here is that a well-exposed signal is close to, but less than, 88% of 65,536—the saturation point of an element on this particular CCD chip. Such a signal in this range is larger than the readout and background noise recorded, but hasn't yet saturated the chip, which would risk losing signal as the chip cannot record more photons. Further analysis of the images shows this estimation to be true. Five zero-bias and five 90-second dark frame images were also collected. These images were used to calibrate and remove instrumental noise from the object images.

3. DATA REDUCTION

The 72 images of the object, plus ten calibration images, were moved to a Sun Ultra 10 Workstation, where they were converted to FITS image files from their native CCD format. Using the IRAF software, the 72 object images were calibrated, using the five zero-bias frames

to remove the individual pixel average bias and the five 90-second dark frames to remove the dark signal from a 90-second exposure of the detector.

Once calibrated, the instrumental V magnitudes of both DY Pegasi and Comp A in each image were determined using the `phot` function. The `phot` function sums the instrumental signal from all pixels that fall within a radius `aperture` from the designated center of the object. The function accounts for partial pixels at the edge of the circle, and subtracts the total average background signal. The background signal is determined by finding the average signal within the circular shell of inner radius `annulus` and outer radius `dannulus` surrounding the object, not including other astronomical objects within this shell. The photometry `aperture` was chosen as 12 pixels and the background sky `annulus` and `dannulus` were set at 17 pixels and 5 pixels, respectively. The instrumental V magnitudes, as determined by IRAF using Equation 1 and an arbitrary "zero point," are recorded in columns D and E of Appendix B. The instrumental V magnitudes of DY Pegasi and Comp A are also graphed in Figure 2.

$$m_{object} - m_0 = -2.5\log_{10}(\frac{S_{object}}{S_0}) \qquad \text{(Equation 1)}$$

The relative V magnitude of DY Pegasi to Comp A for each of the images can be seen in column F of Appendix B. The airmass of Comp A in each image was determined by the `calc-altitude` program (available in the 12.410j locker on Athena, written by Steven Slivan) and an extinction curve solution was calculated using a linear least-squares fit method. Instrumental V magnitude versus airmass is plotted for Comp A in Figure 1. The linear fit, however, was found to be unsuitable since the slope of the derived curve was very close to zero, well below the expected 0.15-0.30 magnitudes per airmass that is expected when observing from Wallace Observatory. This was due to the very small and dense airmass sampling, through which any line

4

would appear well fit. Since the observed stars were beyond transit, and the observation logbook noted no unusual observing conditions, this fit was discarded and the extinction was estimated as a constant, determined by the average of the instrumental V magnitudes for Comp A, which was 12.5687.
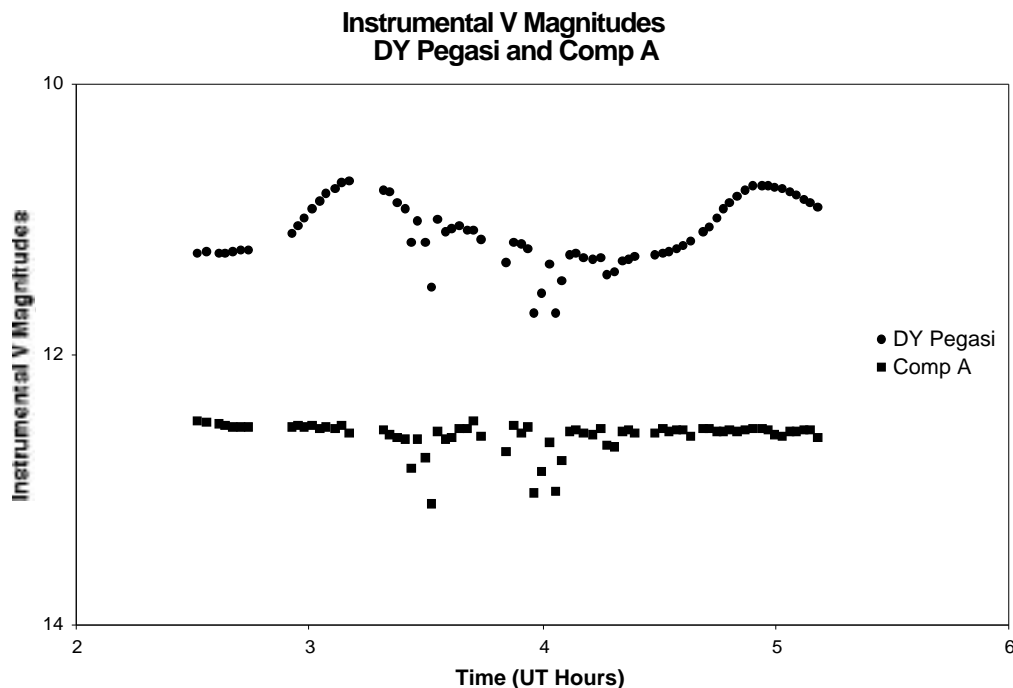

Figure 2. Instrumental V Magnitudes of DY Pegasi and Comp A over time. These are the extracted V magnitudes from IRAF analysis.

Recording the signal from two or more astronomical objects in the same CCD field and then comparing the V magnitudes of the objects to extract a relative V magnitude measurement, using one of the object magnitudes as the zero point, is a technique termed on-chip differential photometry. This technique allows objects to be compared without the need to correct each object magnitude for extinction. Since the field of a CCD is small relative to the sky as a whole, atmospheric effects, such as clouds, usually affect uniformly the signal falling on the pixel array. This technique requires that the response of the CCD pixel array is uniform throughout the field (which was assumed in this case), or that the non-uniformity of the array is known, which can be

accomplished by imaging a flat field with the CCD. This flat field can then be divided out of the object image compensating for the non-uniformity of the CCD array.

DY Pegasi and Comp A both fell into a single field on the CCD pixel array. Since their signals were recorded on the same image frame in each of the 72 images, the light scatter from the presence of clouds affected both signals comparably (note the similar scatter of data points in Figure 2). As a result, when subtracting the V magnitude of DY Pegasi from that of Comp A, the effect of the clouds on the mean signal was removed. At the same time, the clouds increase the intrinsic noise in the mean signal, an effect that cannot be subtracted out.

Using the estimate of constant extinction, the standard deviation of Comp A from the expected value of 12.5687 was determined. The data were separated into three groups of data: images 5-31, images 32-61, and images 62-90. According to the observation logbook, clouds were present in the area of DY Pegasi during the time of UT 3.438-4.309, which corresponds to the second group of images. Note in Figure 2 the scatter of the data points for Comp A during this time. The standard deviation for each of the three groups is shown in Table 1.

Group Number	Image Numbers	Standard Deviation
1	5-31	0.03
2	32-61	0.16
3	62-90	0.02

Table 1. Standard Deviations for Comp A from estimated constant extinction in three groups of images. Note the much larger standard deviation of the second group from the presence of clouds (and therefore data scatter) in the field of the CCD image.

Of note is the significantly higher standard deviation of the middle group of images. These images were the ones affected by the presence of clouds in the field of the CCD. Since the standard deviation of Comp A from the estimated constant extinction was used as a measure for

the intrinsic error in measurement, the images were grouped as above to reduce the estimated error for groups 1 and 3. If there was a single error estimation generated from all 72 images together, the estimated intrinsic error for groups 1 and 3 would have been overestimated due to the increased deviation of group 3 due to clouds.

The standard deviation of Comp A about its mean value was used to estimate the intrinsic error in the measurement of signal of both Comp A and DY Pegasi. Since the signals from the two stars were combined to produce a single relative V magnitude measurement for DY Pegasi, one might assume that the estimated errors from the V magnitude measurements of both DY Pegasi and Comp A should be propagated by adding the squares of the individual standard deviations. This assumption is wrong on two counts: 1) There is no way to successfully derive the standard deviation of the V magnitude of DY Pegasi since that V magnitude is (expectedly) varying with time, and it is exactly that variation that is being measured in this experiment; and 2) The combination of signal from Comp A and DY Pegasi *requires* that the two signals be correlated, and propagation of errors in such a way assumes that the two variables (in this case the two intrinsic V magnitudes) are *not* correlated. The estimated intrinsic error for Comp A was therefore used as an estimated intrinsic error for the relative V magnitude measurements of DY Pegasi.

A second method for estimating the intrinsic error in the measurement of the relative V magnitude of DY Pegasi was used, since the error estimate using the estimated constant extinction drastically overestimated the error of this measurement for the second group of images. Since the cloud cover affected the measurements of intrinsic V magnitude of both DY Pegasi and Comp A, a standard deviation of 0.16 overestimates the error of the relative V magnitude of DY Pegasi when these measurements are combined, especially considering the

small estimated error for the images in groups 1 and 3. Relative V magnitude measurements of DY Pegasi were combined into triplets, averaging three sequential data points and using this average as an estimation for the actual value of the relative V magnitude at the average time of measurement. The triplet-averaged data are shown in Appendix C.

The standard deviation of the three original data points from the triplet averaged data was calculated for all 23 triplet averaged data points. This standard deviation was used as the intrinsic error for the averaged data points. This method of estimating the intrinsic error in the measurement of the relative V magnitude of DY Pegasi assumes that each measurement of the intrinsic V magnitude of DY Pegasi measures the star's actual V magnitude including some error. Since the images were collected sufficiently close to one another in time, three such measurements can be assumed to measure the same quantity, each including some error. By combining these three measurements, the expected error is significantly lower than a single measurement, since the average of the three measurements is a better guess of the actual V magnitude than a single measurement.

This technique of combining three data points into one data point has several drawbacks. First, the amount of data actually encoded in the total amount of averaged data points is lower than the amount of data included in the single measurements, since the light curve is effectively sampled at a much lower frequency. Second, for a light curve that has a high slope—which is the case for the relative V magnitude light curve for DY Pegasi—combining data points that lie along the section of the curve that has a high slope estimates a larger error than actually exists for the data. The magnitude difference from the original data points and the averaged data point is necessarily greater than the magnitude difference for a section of curve that has a small slope.

The two estimated errors were combined to arrive at a final estimate for the intrinsic error for the relative V magnitude of DY Pegasi, shown in column 6 of Appendix B. The estimated constant extinction error was used for data in groups 1 and 3, since this provided a smaller estimated error for data in those groups. This choice seems in line with the quality of the original data collected and shown in Figure 2. The triplet averaged estimated error was used for data in group 2, since this estimation of error was lower than that provided by the estimated constant extinction. This lower error seems accurate, considering that the atmospheric effects that caused variation in the original data affected intrinsic V magnitude measurements of both DY Pegasi and Comp A similarly.

4. ANALYSIS AND RESULTS

Using the relative V magnitude measurements of DY Pegasi, a Fourier series was fitted to the data using Matlab. The program code to produce that fit is included in Appendix C. Note the change from previous versions of the code to return a χ^2 residual instead of a simple residual in line 48 of the program listing for `phit.m`. This change allows the proper weighting of data—dividing by σ—in finding the non-linear least squares fit. The fitted function is shown in Equation 2. A third-order Fourier series was chosen to model the data, since it generated a sufficiently low standard deviation. A higher-order series might provide a lower error when compared to the collected data points, but it risks over-fitting the data points (since they are used both for generating the Fourier series and estimating its error). Over-fitting is undesirable since the data points are assumed to have some error, and therefore deviate from the actual light curve for DY Pegasi by some amount. A Fourier series with too high an order will incorrectly model that error as data. A Fourier series with too low an order does not provide a proper fit for the data.

9

$$y = -1.4805$$
$$-0.190\cos(\frac{2\ t}{1.781}) + 0.158\sin(\frac{2\ t}{1.781})$$
$$+0.039\cos(\frac{4\ t}{1.781}) + 0.072\sin(\frac{4\ t}{1.781}) \qquad \text{(Equation 2)}$$
$$+0.028\cos(\frac{6\ t}{1.781}) - 0.008\sin(\frac{6\ t}{1.781})$$

The estimated extrinsic error of the model fit was calculated using the 72 measurements of DY Pegasi. The standard deviation of the entire series of data points from the model was calculated as 0.0223. This error gives an estimation of the distance of the model from the actual light curve of DY Pegasi, assuming the collected data points fall on this real light curve.

The relative V magnitude of DY Pegasi is shown in Figure 3a. Intrinsic errors are shown as black lines through each data point and extrinsic errors are shown as gray bars through each data point. The curve is the Fourier series model for the data points. Figure 3b shows the relative phase of the data points for DY Pegasi. As can be seen in Figure 3a, both the intrinsic and the extrinsic estimates for the error in measurements and modeling are comparable. Confidence in the result, as well as the collection and processing of data, is therefore high.

The estimated period of DY Pegasi as determined by the Fourier series model is

$$T = 1.7481 \pm 0.04 \ \tfrac{\text{hours}}{\text{cycle}} \qquad \text{(Equation 3)}$$

The error for this period estimate was determined by an empirical estimate, sliding two copies of the light curve in Figure 3a over one another until the error bars no longer fell on the Fourier series curve. A more accurate estimate for the error is unavailable at this time, as the necessary Matlab code to extract the uncertainty in the Fourier series estimate for the period has not been written.

Comparing the results of this experiment to those in other studies of DY Pegasi, such as Wilson, W. J. F. et. al.[2], the data acquired in this experiment seem in line with previous observations of DY Pegasi. Figure 3b shows the same shape as that shown in previous data for DY Pegasi. The previously published period for this star, 1.7502 hours, is well within the empirically estimated error in Equation (3). The derived period is so close to the previously published period for DY Pegasi that the reported error in (3) is likely a large overestimate for the actual error in the measurement. Correct propagation of the error should reveal a much smaller for the period.

Relative V Magnitude vs. Time
DY Pegasi
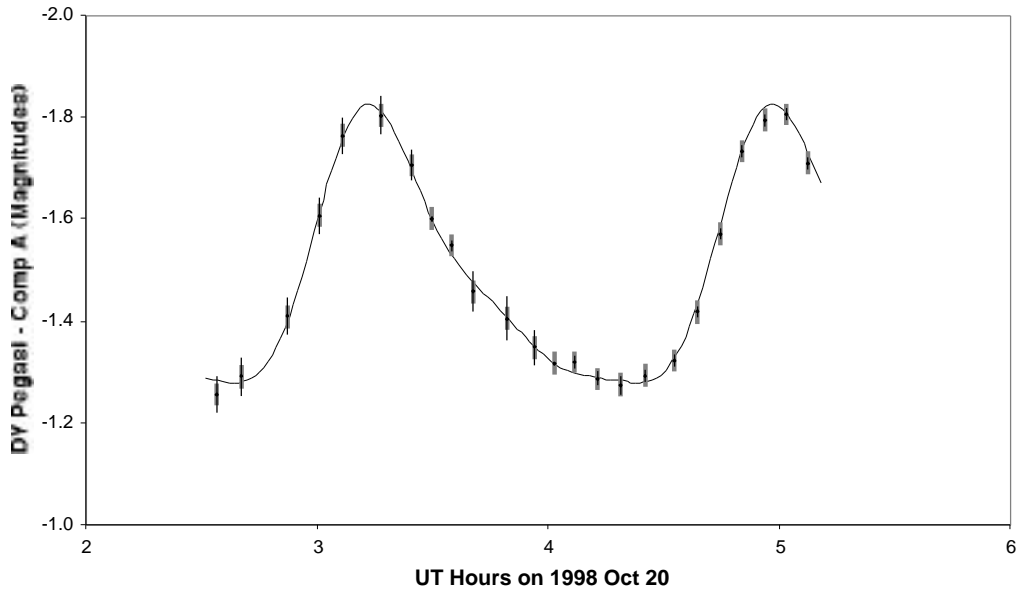
Phase of DY Pegasi
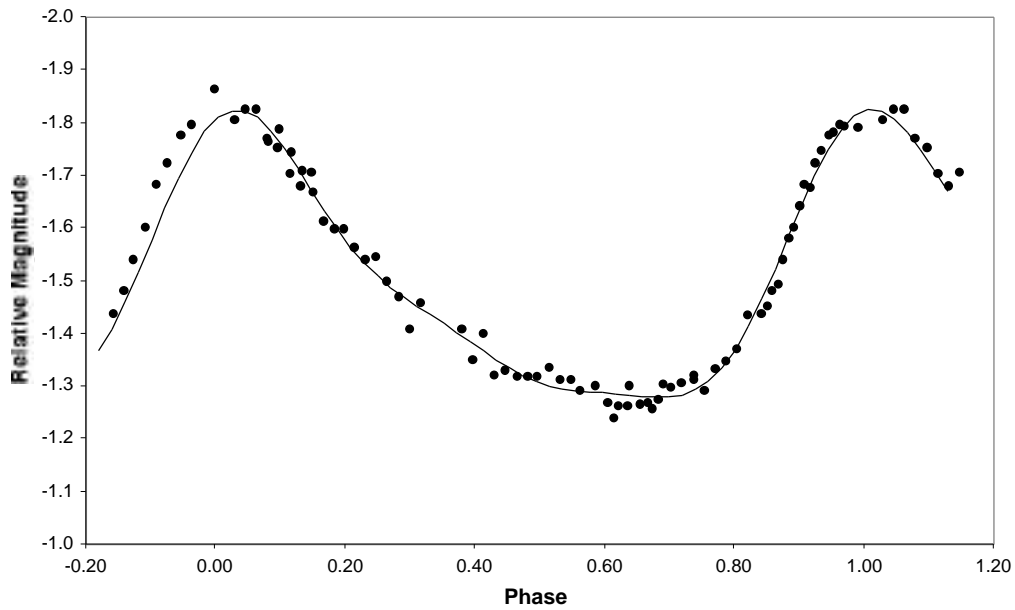
Figure 3a-b. (a) Relative V magnitude of DY Pegasi. Intrinsic errors are shown as black lines through the data points. Extrinsic errors are shown as gray bars through the data points. The Fourier model for DY Pegasi as determined by Matlab is shown as a black curve. (b) Relative phase of DY Pegasi. The Fourier model for DY Pegasi is shown as a black curve.

5. CONCLUSIONS

The period estimation for DY Pegasi represents the conclusion of an extensive process of data reduction and analysis. Observational skills were learned, most notably those of finding a small star field with a CCD camera by star hopping and the proper collection of data for use in a photometric study. During the course of data reduction, the proper method for extracting an intrinsic V magnitude for a celestial body from a CCD image was learned. Final results were derived by learning the proper method of analyzing and graphing the reduced data, and, most importantly, by employing proper error estimation and propagation. In the end, this project was successful on multiple levels, most importantly as a learning experience, but also due to the successful completion of the analysis and the extraction of a result that is in line with prior studies of DY Pegasi.

Further study of DY Pegasi would lead to a more accurate model of the star's V magnitude variability. Also important would be the extraction of error from the Fourier series model fitting stage. This would permit the construction of an accurate estimation of the error in the period derivation.

In principle, the standard V magnitude of DY Pegasi could be determined by performing all-sky photometry, imaging standard stars of known V magnitude as well as DY Pegasi over the course of a night. Knowing the period of V magnitude variation as well as an absolute magnitude would allow a distance estimate of DY Pegasi to be made.

6. REFERENCES

[1] Shu, F. H. (1982) *The Physical Universe: An Introduction to Astronomy.* University Science Books. Sausalito California. 170-171

[2] Wilson, W. J. F., Milone, E. F., Fry, D. J. I., & Leeuwen, J. V. 1998, PASP, 110, 433

7. APPENDIX A – Observing Schedule

Image Number	UT Time hh	mm	ss	special notes
5	2	31	5	
6	2	33	25	
7	2	36	43	
8	2	38	29	
9	2	40	29	
10	2	42	20	
11	2	44	19	
15	2	55	20	
16	2	57	5	
17	2	58	51	
18	3	0	46	
19	3	2	34	
20	3	4	21	
21	3	6	34	
22	3	8	21	
23	3	10	7	
28	3	18	57	
29	3	20	47	
30	3	22	42	
31	3	24	32	
32	3	26	15	clouds in area
33	3	27	58	
34	3	29	42	
35	3	31	26	
36	3	33	11	
37	3	34	57	
38	3	36	42	
39	3	38	27	
40	3	40	28	
41	3	42	14	
42	3	44	2	
46	3	50	48	
47	3	52	43	
48	3	54	28	
49	3	56	16	
50	3	58	0	
51	3	59	51	
52	4	1	39	
53	4	3	20	
54	4	5	11	
55	4	6	58	
56	4	8	44	
57	4	10	29	
58	4	12	58	
59	4	15	1	
60	4	16	46	clouds moving out
61	4	18	33	
62	4	20	22	
63	4	22	10	
64	4	23	57	
68	4	29	3	
69	4	30	51	
70	4	32	40	
71	4	34	32	
72	4	36	17	
73	4	38	4	
74	4	41	13	
75	4	43	1	
76	4	44	46	
77	4	46	32	
78	4	48	17	
79	4	50	4	
80	4	52	5	
81	4	53	57	
82	4	56	22	
83	4	58	9	
84	4	59	54	
85	5	1	41	
86	5	3	33	
87	5	5	23	
88	5	7	18	
89	5	9	5	
90	5	10	54	

8. APPENDIX B – Data Collected

Data extracted and reduced from 72 CCD images with error estimation.

Image Number	Decimal Time	Airmass	Instrumental Magnitude DY Pegasi	Instrumental Magnitude Comp A	Brightness (DY Pegasi-Comp A)	Extinction Fit (constant)	Residual from Extinction	Extinction Standard Deviation	Fourier Model	Fourier Model Residual	Fourier Model Standard Deviation
5	2.518	1.115	11.247	12.487	-1.240	12.57	-0.08	0.03	-1.29	0.05	0.02
6	2.557	1.116	11.242	12.504	-1.262	12.57	-0.06	0.03	-1.28	0.02	0.02
7	2.612	1.118	11.249	12.517	-1.268	12.57	-0.05	0.03	-1.28	0.01	0.02
8	2.641	1.119	11.248	12.522	-1.274	12.57	-0.05	0.03	-1.28	0.01	0.02
9	2.675	1.12	11.237	12.533	-1.296	12.57	-0.04	0.03	-1.28	-0.02	0.02
10	2.706	1.122	11.23	12.536	-1.306	12.57	-0.03	0.03	-1.28	-0.02	0.02
11	2.739	1.123	11.226	12.537	-1.311	12.57	-0.03	0.03	-1.29	-0.02	0.02
15	2.922	1.132	11.099	12.536	-1.437	12.57	-0.03	0.03	-1.46	0.03	0.02
16	2.951	1.134	11.045	12.527	-1.482	12.57	-0.04	0.03	-1.51	0.03	0.02
17	2.981	1.136	10.993	12.532	-1.539	12.57	-0.04	0.03	-1.56	0.02	0.02
18	3.013	1.138	10.926	12.528	-1.602	12.57	-0.04	0.03	-1.61	0.01	0.02
19	3.043	1.14	10.864	12.547	-1.683	12.57	-0.02	0.03	-1.66	-0.02	0.02
20	3.073	1.142	10.807	12.529	-1.722	12.57	-0.04	0.03	-1.71	-0.02	0.02
21	3.109	1.144	10.775	12.551	-1.776	12.57	-0.02	0.03	-1.75	-0.02	0.02
22	3.139	1.146	10.724	12.521	-1.797	12.57	-0.05	0.03	-1.78	-0.01	0.02
23	3.169	1.148	10.712	12.574	-1.862	12.57	0.01	0.03	-1.81	-0.06	0.02
28	3.316	1.16	10.788	12.552	-1.764	12.57	-0.02	0.03	-1.79	0.02	0.02
29	3.346	1.162	10.801	12.589	-1.788	12.57	0.02	0.03	-1.76	-0.03	0.02
30	3.378	1.165	10.875	12.618	-1.743	12.57	0.05	0.03	-1.73	-0.01	0.02
31	3.409	1.168	10.92	12.629	-1.709	12.57	0.06	0.03	-1.70	-0.01	0.02
32	3.438	1.17	11.173	12.842	-1.669	12.57	0.27	0.16	-1.67	0.00	0.02
33	3.466	1.173	11.01	12.621	-1.611	12.57	0.05	0.16	-1.63	0.02	0.02
34	3.495	1.176	11.167	12.766	-1.599	12.57	0.20	0.16	-1.60	0.01	0.02
35	3.524	1.179	11.505	13.102	-1.597	12.57	0.53	0.16	-1.58	-0.02	0.02
36	3.553	1.182	11.001	12.565	-1.564	12.57	0.00	0.16	-1.55	-0.01	0.02
37	3.583	1.185	11.089	12.628	-1.539	12.57	0.06	0.16	-1.53	-0.01	0.02
38	3.612	1.188	11.066	12.612	-1.546	12.57	0.04	0.16	-1.51	-0.04	0.02
39	3.641	1.191	11.046	12.545	-1.499	12.57	-0.02	0.16	-1.49	-0.01	0.02
40	3.674	1.195	11.074	12.544	-1.470	12.57	-0.02	0.16	-1.48	0.01	0.02
41	3.704	1.198	11.083	12.49	-1.407	12.57	-0.08	0.16	-1.46	0.05	0.02
42	3.734	1.201	11.146	12.605	-1.459	12.57	0.04	0.16	-1.45	-0.01	0.02
46	3.847	1.215	11.314	12.721	-1.407	12.57	0.15	0.16	-1.40	-0.01	0.02
47	3.879	1.219	11.168	12.519	-1.351	12.57	-0.05	0.16	-1.38	0.03	0.02
48	3.908	1.223	11.185	12.584	-1.399	12.57	0.02	0.16	-1.37	-0.03	0.02
49	3.938	1.227	11.213	12.535	-1.322	12.57	-0.03	0.16	-1.35	0.03	0.02
50	3.967	1.231	11.691	13.019	-1.328	12.57	0.45	0.16	-1.34	0.01	0.02
51	3.998	1.235	11.548	12.867	-1.319	12.57	0.30	0.16	-1.33	0.01	0.02
52	4.028	1.24	11.33	12.648	-1.318	12.57	0.08	0.16	-1.32	0.00	0.02
53	4.056	1.244	11.689	13.006	-1.317	12.57	0.44	0.16	-1.31	-0.01	0.02
54	4.086	1.248	11.452	12.788	-1.336	12.57	0.22	0.16	-1.30	-0.03	0.02
55	4.116	1.253	11.262	12.573	-1.311	12.57	0.00	0.16	-1.30	-0.01	0.02
56	4.146	1.257	11.249	12.562	-1.313	12.57	-0.01	0.16	-1.29	-0.02	0.02
57	4.175	1.262	11.281	12.574	-1.293	12.57	0.01	0.16	-1.29	0.00	0.02
58	4.216	1.268	11.291	12.591	-1.300	12.57	0.02	0.16	-1.29	-0.01	0.02
59	4.250	1.274	11.279	12.548	-1.269	12.57	-0.02	0.16	-1.29	0.02	0.02
60	4.279	1.279	11.41	12.671	-1.261	12.57	0.10	0.16	-1.28	0.02	0.02
61	4.309	1.284	11.382	12.683	-1.301	12.57	0.11	0.16	-1.28	-0.02	0.02
62	4.339	1.289	11.305	12.57	-1.265	12.57	0.00	0.02	-1.28	0.02	0.02
63	4.369	1.295	11.296	12.554	-1.258	12.57	-0.01	0.02	-1.28	0.02	0.02
64	4.399	1.3	11.272	12.575	-1.303	12.57	0.01	0.02	-1.28	-0.02	0.02
68	4.484	1.316	11.26	12.58	-1.320	12.57	0.01	0.02	-1.29	-0.03	0.02
69	4.514	1.322	11.251	12.542	-1.291	12.57	-0.03	0.02	-1.30	0.01	0.02
70	4.544	1.328	11.235	12.566	-1.331	12.57	0.00	0.02	-1.32	-0.01	0.02
71	4.576	1.334	11.214	12.561	-1.347	12.57	-0.01	0.02	-1.35	0.00	0.02
72	4.605	1.34	11.192	12.562	-1.370	12.57	-0.01	0.02	-1.38	0.01	0.02
73	4.634	1.347	11.164	12.599	-1.435	12.57	0.03	0.02	-1.41	-0.02	0.02
74	4.687	1.358	11.096	12.547	-1.451	12.57	-0.02	0.02	-1.49	0.04	0.02
75	4.717	1.365	11.057	12.55	-1.493	12.57	-0.02	0.02	-1.54	0.05	0.02
76	4.746	1.371	10.99	12.571	-1.581	12.57	0.00	0.02	-1.59	0.01	0.02
77	4.776	1.378	10.926	12.568	-1.642	12.57	0.00	0.02	-1.64	-0.01	0.02
78	4.805	1.385	10.879	12.556	-1.677	12.57	-0.01	0.02	-1.68	0.00	0.02
79	4.834	1.392	10.826	12.571	-1.745	12.57	0.00	0.02	-1.72	-0.02	0.02
80	4.868	1.4	10.781	12.562	-1.781	12.57	-0.01	0.02	-1.77	-0.02	0.02
81	4.899	1.408	10.753	12.545	-1.792	12.57	-0.02	0.02	-1.79	0.00	0.02
82	4.939	1.418	10.754	12.543	-1.789	12.57	-0.03	0.02	-1.82	0.03	0.02
83	4.969	1.426	10.749	12.553	-1.804	12.57	-0.02	0.02	-1.82	0.02	0.02
84	4.998	1.434	10.767	12.591	-1.824	12.57	0.02	0.02	-1.82	0.00	0.02
85	5.028	1.442	10.772	12.597	-1.825	12.57	0.03	0.02	-1.81	-0.01	0.02
86	5.059	1.45	10.799	12.57	-1.771	12.57	0.00	0.02	-1.79	0.02	0.02
87	5.090	1.459	10.822	12.573	-1.751	12.57	0.00	0.02	-1.77	0.02	0.02
88	5.122	1.468	10.856	12.558	-1.702	12.57	-0.01	0.02	-1.74	0.03	0.02
89	5.151	1.477	10.879	12.558	-1.679	12.57	-0.01	0.02	-1.70	0.02	0.02
90	5.182	1.486	10.908	12.613	-1.705	12.57	0.04	0.02	-1.67	-0.03	0.02

Triplet data with error estimation.

Decimal Time	Triplet Averaged Relative Magnitude	Triplet Standard Deviation	Extinction Residual	Extinction Standard Deviation	combined error	Notes
2.562	-1.257	0.012	-0.066	0.037	0.037	error from extintion
2.674	-1.292	0.013	-0.038	0.037	0.037	
2.871	-1.410	0.072	-0.035	0.037	0.037	
3.012	-1.608	0.059	-0.033	0.037	0.037	
3.107	-1.765	0.032	-0.035	0.037	0.037	
3.277	-1.805	0.042	0.043	0.037	0.037	
3.408	-1.707	0.030	0.128	0.098	0.030	error from triplet
3.495	-1.602	0.006	0.261	0.098	0.006	
3.582	-1.550	0.011	0.033	0.098	0.011	
3.673	-1.459	0.038	-0.042	0.098	0.038	
3.820	-1.406	0.044	0.046	0.098	0.044	
3.937	-1.350	0.035	0.144	0.098	0.035	
4.027	-1.318	0.001	0.238	0.098	0.001	
4.116	-1.320	0.011	0.072	0.098	0.011	
4.214	-1.287	0.013	0.002	0.098	0.013	
4.309	-1.276	0.018	0.073	0.098	0.018	
4.418	-1.294	0.026	0.001	0.011	0.011	error from extintion
4.545	-1.323	0.024	-0.012	0.011	0.011	
4.642	-1.419	0.035	0.001	0.011	0.011	
4.746	-1.572	0.061	-0.006	0.011	0.011	
4.836	-1.734	0.043	-0.006	0.011	0.011	
4.936	-1.795	0.006	-0.022	0.011	0.011	
5.029	-1.807	0.025	0.017	0.011	0.011	
5.121	-1.711	0.030	-0.006	0.011	0.011	

9. APPENDIX C – Non-linear Least Squares Fourier Series Fit Program Listing for MATLAB

```
1  function f = phit(lam,Data)
2  %PHIT  Used  to return errors in fitting data to a function.
3  %        PHIT(lam,Data) returns the error
4  %        between the data and the values computed by the current
5  %        function of lam.  PHIT assumes a function of the form
6  %
7  %          y =  c(1) + c(2)*cos((2*pi*1)*t/lam(1)) +
8  %                      c(3)*sin((2*pi*1)*t/lam(1)) +
9  %                      ... +
10 %                      c(2*order)*cos((2*pi*order)*t/lam(1)) +
11 %                      c(2*order+1)*sin((2*pi*order)*t)/lam(1))
12 %
13 %        with (2*order+1) linear parameters 'c(n)' and
14 %        1 nonlinear parameter 'lam(1)' (the period P)
15 %
16
17 order = 3; % selects how many harmonics to include in fit
18
19 t = Data(:,1);
20 y = Data(:,2);
21 sig = Data(:,3);
22
23 A = zeros(length(t),2*order+1);
24 % A will be the "design matrix" of <N = number of data> rows by
25 % <M = number of linear coefficients> columns.  It contains
26 % the values of M basis functions evaluated at the N abscissas
27 % (note: for now sigmas are not used)
28
29 % c(1) is a constant term, so the first column of A is all 1's
30 A(:,1) = ones(length(t),1);
31
32 % the rest of the c(n) are the cos and sin terms
33 for j = 1:order
34    k = (j*2);
35      A(:,k) = cos((2*pi*j)*t/lam(1));
36      A(:,k+1) = sin((2*pi*j)*t/lam(1));
37 end
38
39 % c = A\y is the solution in the least squares sense to the
40 % overdetermined system of equations A*c = y.
41 c = A\y;
42
43 % z is vector of fitted values
44 z = A*c;
45
46 % f is vector of fit residuals z-y. This should be a Chi-Square statistic
47 % f = z-y;
48 f = (z-y)./sig;
49
50 % Statements to plot progress of fitting:
51 plot(t,z,'-g',t,y,'o')
52 xt = min(t)+(max(t)-min(t))/10;
53 yt = (max(y)-min(y))/11.0;
```

```
54 text(xt,max(y)-1*yt,['order = ' num2str(order)])
55 text(xt,max(y)-2*yt,['period = ' sprintf('%.4f',lam(1))])
56text(xt,max(y)-3*yt,['sigma of fit = ' sprintf('%.3f',sqrt(sum(f.^2)/(length(f))))])
57 text(xt,max(y)-4*yt,['c1=' sprintf('%.4f',c(1))])
58
59 if order >= 1
60 text(xt,max(y)-5*yt,['c2=' sprintf('%.3f',c(2)) ' c3=' sprintf('%.3f',c(3))])
61 end
62
63 if order >= 2
64 text(xt,max(y)-6*yt,['c4=' sprintf('%.3f',c(4)) ' c5=' sprintf('%.3f',c(5))])
65 end
66
67 if order >= 3
68 text(xt,max(y)-7*yt,['c6=' sprintf('%.3f',c(6)) ' c7=' sprintf('%.3f',c(7))])
69 end
70
71 if order >= 4
72 text(xt,max(y)-8*yt,['c8=' sprintf('%.3f',c(8)) ' c9=' sprintf('%.3f',c(9))])
73 end
74
75 if order >= 5
76 text(xt,max(y)-9*yt,['c10=' sprintf('%.3f',c(10)) ' c11=' sprintf('%.3f',c(11))])
77 end
78
79 if order >= 6
80 text(xt,max(y)-10*yt,['c12=' sprintf('%.3f',c(12)) ' c13=' sprintf('%.3f',c(13))])
81 end
82
83 if order >= 7
84 text(xt,max(y)-11*yt,['c14=' sprintf('%.3f',c(14)) ' c15=' sprintf('%.3f',c(15))])
85 end
```